J. Fluid Mech. (2002), *vol.* 460, *pp.* 39–56.
DOI: 10.1017/S0022112002008194 Printed in the United Kingdom

Expansion dynamics of volatile-supersaturated liquids and bulk viscosity of bubbly magmas

By N. G. LENSKY[1], V. LYAKHOVSKY[2] AND O. NAVON[1]

[1]Institute of Earth Sciences, The Hebrew University, Jerusalem 91904, Israel

[2]Geological Survey of Israel, 30 Malkhe Yisrael St., Jerusalem 95501, Israel
e-mail: nadavl@vms.huji.ac.il

(Received 8 September 2000 and in revised form 9 November 2001)

We derive expressions for the bulk viscosity of suspension of gas bubbles in an incompressible Newtonian liquid that exsolves volatiles. The suspension is modelled as close packed spherical cells and is represented by a single cell ('cell model'). A cell, consisting of a gas bubble centred in a spherical shell of a volatile-bearing liquid, is subjected to decompression that is applied at the cell boundary, and the resulting dilatational boundary motion and driving pressure are obtained. The dilatational motion and the driving pressure are used to define the bulk viscosity of the cell, as if it were composed of a homogeneously compressible fluid. By definition, the bulk viscosity is the relation between changes of the driving pressure and changes in the resulting expansion strain rate. The bulk viscosity of the suspension is obtained in terms of two-phase parameters, i.e. bubble radius, gas pressure and the properties of the incompressible continuous liquid phase. The resulting bulk viscosity is highly nonlinear. At the beginning of the expansion process, when gas exsolution is efficient, the expansion rate grows exponentially while the driving pressure decreases slightly, which means that the bulk viscosity is formally negative. This negative value reflects the release of the energy stored in the supersaturated liquid and its transfer to mechanical work during exsolution. Later, when bubbles are large and the gas influx decreases significantly, the strain rate decelerates and the bulk viscosity becomes positive as expected in a dissipative system. We demonstrate that amplification of seismic waves travelling through a volcanic conduit filled with a volatile saturated magma may be attributed to the negative bulk viscosity of the compressible magma. Amplification of an expansion wave may, at some level in the conduit, damage the conduit walls and initiate the opening of a new pathway for magma eruption. We also consider the energy related to positive and negative bulk viscosities.

1. Introduction

Bulk viscosity is a physical property of compressible fluids that relates the changes in applied stresses to the resultant change in expansion strain rate (Malvern 1969). Suspensions of gas bubbles that are trapped in a continuous incompressible liquid phase may be regarded as a uniformly compressible fluid. Several expressions for the bulk viscosity of such suspensions, assuming constant mass of the gas in the bubbles, have been derived. Using the procedure of averaging of periodic structures of a multi-phase material, which is widely applied to estimate effective properties of composite materials (e.g. Christensen 1979), Taylor (1954) derived an expression for

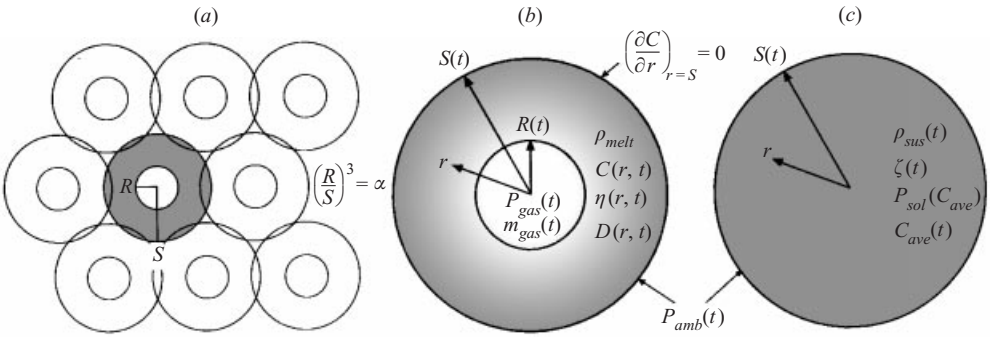

FIGURE 1. Cell models of a gas–liquid suspension (magma). P_{gas} – gas pressure; P_{amb} – ambient pressure; P_{sol} – solubility pressure; R – bubble radius; S – cell radius; r – radial coordinate; t – time; α – gas volume fraction; C – volatile concentration (mass fraction); C_{ave} – average volatile concentration in the liquid shell; ρ_{liq} – liquid density; ρ_{sus} – density of the suspension (the cell); m_{gas} – mass of gas in the bubble (increases with time); η – shear viscosity of the liquid; ζ – bulk viscosity of the liquid. (*a*) A pack of spherical cells, each composed of a gas bubble with radius R centred in a spherical liquid shell with outer radius S. The cells are arranged in a three-dimensional lattice with some overlap, so that gas volume fraction is $\alpha = (R/S)^3$. (*b*) A two-phase cell containing an expanding gas bubble in an incompressible viscous liquid shell. The liquid is oversaturated in dissolved volatiles, but at the liquid–bubble interface volatiles are transferred into the bubble and local equilibrium is attained (equation (3.7)). (*c*) One-phase cell containing a single compressible fluid. The properties of the fluid are uniform throughout the cell, but vary with time so they represent the effective properties of the two-phase cell.

the effective bulk viscosity, ζ, of such a suspension:

$$\zeta = \frac{4}{3}\frac{\eta}{\alpha}, \tag{1.1}$$

where the volume fraction of gas is low ($\alpha \ll 1$) and the shear viscosity of the liquid, η, is Newtonian. For infinitely small gas volume fraction the bulk viscosity goes to infinity, as in the incompressible liquid. Later studies refined the expression for the bulk viscosity of similar suspensions by accounting for higher gas volume fraction (Prud'homme & Bird 1978). The suspension was regarded as close packed spherical cells, each cell containing a spherical bubble surrounded by a viscous liquid shell (figure 1). The pressure at the boundary of the cell was calculated twice: in the 'actual' two-phase cell and in an equivalent cell containing a single compressible phase of unknown viscosity. Equating the pressures and the strain rates in the two cells yielded the bulk viscosity of the non-dilute suspension, which is smaller than equation (1.1) by a factor of $1-\alpha$. Prud'homme & Bird (1978) and Aksel (1995) also derived expressions for the bulk viscosity of similar suspensions of non-Newtonian liquids using a cell model. These cases with no volatile mass flux are applicable to the field of processing technology, e.g. when gas bubbles are introduced and trapped in water or in polymer liquids.

In many cases transfer of volatiles into the bubbles cannot be ignored. For example, explosive volcanic eruptions, one of the most energetic phenomena on Earth, are driven by gas exsolution from a supersaturated melt into bubbles. This expands the volume of the magma by up to a factor of four, accelerates the bubbly magma, fragments it into pumice and ash and accelerates them to near-sonic or supersonic velocities (Woods 1995). Examples of such eruptions include Santorini (Greece, $\sim$ 1600 BC), Mt. St. Helens (USA, 1980), Pinatubo (Philippines, 1991). Less energetic eruptions lead to lava flows, as in low-viscosity basalt effusing on Hawaii, or if the magma

is more viscous, to the formation of lava domes as in the case of Mt. St. Helens late activity during 1981–1986; Mt. Unzen (Japan, 1991–1993) and the present eruptions of the Soufrière Hills (Montserrat, 1995 to present) and Popocatepetl (Mexico, 1998 to present). These lava domes are unstable and in many cases gravitational collapse may trigger an explosive eruption. Treating the active magmatic conduit as a uniformly compressible fluid of well-characterized effective properties facilitates modelling of the phenomenon. Such an approach is useful in modelling the dynamics of flow in the conduit (e.g. Massol & Jaupart 1999). It is also important for modelling the interaction of the magma-filled conduit with seismic waves. The bulk viscosity of the compressible fluid is the least known property, but is essential for quantifying these effects.

In this paper we examine the bulk viscosity of a compressible bubbly suspension where exsolution of volatiles drives expansion. We obtain the expression for the bulk viscosity using its definition: the differential relation between the driving pressure and the expansion strain rate. This approach is an extension of previous models mentioned above, and yields the same results in the condition of no gas flux.

2. The physical model

2.1. *The suspension*

We consider a suspension of equally sized and evenly distributed gas bubbles in an incompressible liquid. The suspension is divided into closely packed non-interacting cells. Each cell is spherical and consists of a stationary gas bubble centred in a spherical liquid shell (figure 1). The cells are arranged so that the volume fraction of the suspension, α, equals the volume fraction of a bubble of radius R in a cell of radius S:

$$\alpha = \frac{R^3}{S^3}. \tag{2.1}$$

The liquid is Newtonian and incompressible, and its volume ($4\pi S_0^3/3$) is conserved; the subscript zero denotes the state where the bubble vanishes ($R \to 0$). The total volume of the cell is $4\pi S^3/3 = 4\pi(S_0^3 + R^3)/3$. The liquid dissolves volatiles as a function of pressure. Following decompression, the liquid becomes supersaturated, bubbles nucleate and grow and consequently the suspension undergoes dilatational motion. We assume a single nucleation event. The expansion kinetics is limited by the viscous resistance of the liquid shell and the diffusion of volatiles through the liquid into the bubble.

Each cell in the suspension is a closed system and no mass is allowed to escape from the cell boundary. Volatile mass flux is allowed between the liquid and the gas bubble. The pressure at the boundary of each cell is the ambient pressure of the suspension, i.e. the bubbles do not interact mechanically. Under these conditions, the dilatational behaviour and properties of a single cell are identical to those of the whole suspension. Treating the suspension as a single cell with spherical symmetry simplifies the mathematical formulation to a one-dimensional (radial) model.

The effective bulk viscosity of such a suspension is obtained by treating it as a homogeneously compressible fluid (figure 1). This approach is justified when the diameter of the cells is much shorter than the diameter of the conduit through which the suspension flows or the wavelength of acoustic waves that travel through the suspension.

2.2. *Pressures in the suspension*

To understand the pressures in the expanding suspension, we first consider a simpler system where there is no volatile mass exchange between bubbles and the liquid. Following decompression, the suspension expands until the gas pressure in the bubbles is in balance with the ambient pressure and stress due to surface tension, $P_{gas} = P_{amb} + P_{surf}$. The transient pressure that drives expansion of the non-exsolving suspension is $P_{drive} = P_{gas} - P_{amb} - P_{surf}$. During the transient stage, the driving pressure is equal to the viscous resistance of the liquid shell, $P_{drive} = P_{visc}$. Thus, at any given moment during expansion, if P_{amb} is elevated to equate with $P_{gas} - P_{surf}$, the system equilibrates mechanically and expansion ceases.

In the more complex system, where volatile mass flux is allowed, elevating P_{amb} to equate with $P_{gas} - P_{surf}$ is not sufficient to ensure equilibrium. If the melt is supersaturated with respect to P_{gas}, volatile influx and bubble expansion will continue. Mass flux ceases only if chemical equilibrium is also satisfied. For that, P_{amb} should be elevated to the solubility pressure, P_{sol}, which is in equilibrium with the supersaturated liquid and higher than with P_{gas}. This pressure is related to the average volatile concentration in the liquid shell, C_{ave}, through Henry's solubility law:

$$P_{sol} = \left(\frac{C_{ave}}{K_H}\right)^n = P_0 \left(\frac{C_{ave}}{C_0}\right)^n, \tag{2.2}$$

where K_H is Henry's constant, n depends on the nature of the liquid and volatile species, P_0 and C_0 refer to the saturation pressure and concentration respectively (then $R = 0$). When $P_{sol} - P_{amb} = 0$, chemical equilibrium is established immediately and mechanical equilibrium is reached shortly after. The pressure driving the expansion of the exsolving suspension is the difference between the thermodynamic solubility pressure and the ambient pressure:

$$P_{drive} = P_{sol} - P_{amb}.$$

2.3. *The hydrodynamics of an expanding compressible fluid – the one-phase cell*

At the macroscopic scale, the suspension is regarded as a uniformly compressible fluid (§ 2.1). The model accounts for the equation of continuity and the equation of motion of the compressible fluid. All equations are written with spherical symmetry and assuming isothermal conditions.

The equation of continuity is

$$\frac{\partial \rho_{sus}}{\partial t} + \frac{1}{r^2}\frac{\partial}{\partial r}(\rho_{sus} r^2 v_{sus}) = 0, \tag{2.3}$$

where v_{sus} is the radial velocity in the cell and ρ_{sus} is the average density of the suspension. Using the 'actual' structure of the fluid (figure 1), the density of the cell, ρ_{sus}, is the mass of the cell, m_{sus}, divided by its volume:

$$\rho_{sus} = \frac{m_{sus}}{\frac{4}{3}\pi S^3}. \tag{2.4}$$

Substitution of (2.4) into (2.3) yields the divergence of the velocity field which is the expansion strain rate:

$$\operatorname{div} \boldsymbol{v}_{sus} = \frac{1}{r^2}\frac{\partial (r^2 v_{sus})}{\partial r} = 3\frac{\dot{S}}{S}, \tag{2.5}$$

where the overdot denotes the time derivative. The resulting expansion strain rate

(2.5) is independent of the radial coordinate, and thus is uniform throughout the fluid. The uniform strain rate and the homogeneity of the fluid mean that the stress tensor is also uniform. Thus, the equation of fluid motion in spherical symmetry (neglecting inertial terms),

$$-\frac{1}{r^2}\frac{\partial}{\partial r}(r^2\sigma_{rr}) + \frac{\sigma_{\theta\theta} + \sigma_{\phi\phi}}{r} = 0, \tag{2.6}$$

is reduced to

$$\sigma_{rr} = \sigma_{\theta\theta} = \sigma_{\phi\phi}, \tag{2.7}$$

where σ_{rr}, $\sigma_{\theta\theta}$, and $\sigma_{\phi\phi}$ are components of the total stress tensor in spherical coordinates. The total stress components consist of the fluid thermodynamic (solubility) pressure, P_{sol}, and the stresses driving expansion (see § 2.2):

$$\sigma_{rr} = -P_{sol} + P_{drive}. \tag{2.8}$$

The total stress acting at the cell surface is P_{amb}:

$$\sigma_{rr}|_{r=S} = -P_{amb}. \tag{2.9}$$

Thus, the driving pressure is the difference between solubility and ambient pressures:

$$P_{drive} = P_{sol} - P_{amb}. \tag{2.10}$$

The definition of bulk viscosity, following Malvern (1969), accounts for nonlinear constitutive relations of the expanding fluid; it is the differential relation between the driving pressure (2.10) and the strain rate (2.5):

$$\zeta = \frac{\partial(P_{drive})}{\partial(\operatorname{div} \boldsymbol{v}_{sus})}. \tag{2.11}$$

2.4. *Bulk viscosity of the suspension in terms of the bubble growth dynamics*

We wish to express bulk viscosity (2.11) in terms of the 'actual' two-phase cell model parameters ($R(t)$, α and gas density $\rho_{gas}(t)$). First we substitute equation (2.1) into (2.5) and obtain the expansion strain rate of the one-phase cell in terms of the bubble radius and gas volume fraction:

$$\operatorname{div} \boldsymbol{v}_{sus} = 3\frac{\dot{R}}{R}\alpha. \tag{2.12}$$

The differential of the expansion strain rate (2.12) is

$$\mathrm{d}(\operatorname{div} \boldsymbol{v}_{sus}) = \left\{ 3\frac{\dot{R}}{R}\alpha \left[\frac{\ddot{R}}{\dot{R}} + \frac{\dot{R}}{R}(2 - 3\alpha) \right] \right\} \mathrm{d}t. \tag{2.13}$$

To obtain the driving pressure in terms of the two-phase parameters, we express the solubility pressure (or C_{ave}) in terms of the concentration of volatiles in the liquid. The equation of mass conservation of volatiles in the cell relates the mass of gas in the bubble to the difference between the initial volatile concentration (C_0) and the remaining average volatile concentration (C_{ave}):

$$\tfrac{4}{3}\pi R^3 \rho_{gas} = \tfrac{4}{3}\pi S_0^3 \rho_{liq}(C_0 - C_{ave}), \tag{2.14}$$

where ρ_{gas} is the density of the gas and ρ_{liq} is the density of the incompressible liquid. Substituting (2.2) into (2.14), yields the equation for the solubility pressure:

$$P_{sol} = P_0(1 - \delta)^n, \tag{2.15}$$

where δ is the mass fraction of volatile in the bubble from the total volatile mass:

$$\delta = \frac{R^3 \rho_{gas}}{S_0^3 \rho_{melt} C_0}, \quad 0 < \delta \leqslant \frac{C_0 - K_H P_{amb}^{1/n}}{C_0} < 1. \tag{2.16}$$

P_{sol} (and C_{ave}) decrease during exsolution from the initial saturation pressure (P_0) to P_{amb}. The maximum δ-value is reached when the volatile content in the liquid is in equilibrium with ambient pressure.

Substitution of (2.15) and (2.16) into (2.10) and differentiation yields the derivative of the driving stress of expansion:

$$\mathrm{d}(P_{drive}) = \mathrm{d}(P_{sol} - P_{amb}) = \left[P_0 n (1-\delta)^{n-1} \delta \left(3\frac{\dot{R}}{R} + \frac{\dot{\rho}_{gas}}{\rho_{gas}} \right) + \dot{P}_{amb} \right] \mathrm{d}t. \tag{2.17}$$

Substituting (2.13) and (2.17) into (2.11) yields

$$\zeta = -\frac{P_0 n (1-\delta)^{n-1} \delta \left(3\frac{\dot{R}}{R} + \frac{\dot{\rho}_{gas}}{\rho_{gas}} \right) + \dot{P}_{amb}}{3\frac{\dot{R}}{R}\alpha \left[\frac{\ddot{R}}{\dot{R}} + \frac{\dot{R}}{R}(2 - 3\alpha) \right]}. \tag{2.18}$$

Equation (2.18) is a general expression which allows the calculation of bulk viscosity of a suspension with the known bubble growth parameters: $R(t)$, $\alpha(t)$, $\rho_{gas}(t)$ and $P_{amb}(t)$.

2.5. *Dynamics of bubble growth – two-phase cell*

To solve the evolution of the bubble size and gas density in an exsolving suspension, we adopt a bubble growth model that is based on the formulation of Rayleigh (1917). We use a modified model that accounts for the requirements of a volatile-dissolving system (Proussevitch, Sahagian & Anderson 1993; Lyakhovsky, Hurwitz & Navon 1996).

The equations of continuity and motion of the incompressible viscous liquid within the spherical shell ($R < r < S$) are

$$\frac{1}{r^2}\frac{\partial}{\partial r}(r^2 v_{liq}) = 0, \tag{2.19}$$

$$-\frac{\partial P}{\partial r} + \frac{1}{r^2}\frac{\partial}{\partial r}\left(2\eta r^2 \frac{\partial v_{liq}}{\partial r} \right) - \frac{4\eta v_{liq}}{r^2} = 0, \tag{2.20}$$

where v_{liq} is the radial velocity in the liquid shell and (η is its Newtonian shear viscosity, which is radially variable. We neglect the changes of liquid density with variations of volatile content. These are common assumptions in the case of water-bearing silicic melts where density changes only by 2% upon addition of 10 mole percent of water (Dingwell 1998). Inertial terms in the equation of motion are neglected, as the Reynolds number is typically small ($Re \equiv \dot{R} S \rho_{liq}/\eta \ll 1$).

The equation of continuity is integrated to obtain the velocity distribution in the liquid phase:

$$v_{liq} = \dot{R} R^2 \frac{1}{r^2} \quad (R < r < S). \tag{2.21}$$

The pressure in the fluid at the gas bubble interface is balanced by the gas pressure

and surface tension:

$$-P(R) + 2\eta \left(\frac{\partial v_{liq}}{\partial r} \right)_{r=R} = -P_{gas} + P_{surf}. \tag{2.22}$$

The pressure in the fluid at the boundary of the cell equals the ambient pressure:

$$-P(S) + 2\eta \left(\frac{\partial v_{liq}}{\partial r} \right)_{r=S} = -P_{amb}(t). \tag{2.23}$$

Integrating the equation of motion (2.20), using (2.21), and the boundary conditions (2.22) and (2.23), yields

$$P_{visc} = 4\frac{\dot{R}}{R}\eta_{eff} = P_{gas} - P_{amb} - P_{surf}, \tag{2.24a}$$

where the effective Newtonian viscosity, η_{eff}, resisting the growth of bubbles (Lensky, Lyakhovsky & Navon 2001) is

$$\eta_{eff} = 3R^3 \int_R^S \frac{\eta}{r^4} \mathrm{d}r. \tag{2.24b}$$

Equation (2.24*a*) relates gas pressure to the bubble radius. To solve for these two quantities, we need another equation containing information on gas pressure and/or bubble size. The information comes from the rate of volatile mass accumulation in the bubble by the mass flux through the bubble–liquid interface:

$$\frac{4\pi}{3}\frac{\mathrm{d}}{\mathrm{d}t}(\rho_{gas}R^3) = 4\pi R^2 \rho_{liq} D \left. \frac{\partial C}{\partial r} \right|_{r=R}, \tag{2.25}$$

where D is volatile diffusivity in the liquid and C is the weight fraction of volatiles in the liquid. The gas is assumed to be ideal, thus gas density is proportional to gas pressure through the equation of state:

$$\rho_{gas} = P_{gas}\frac{M}{GT}, \tag{2.26}$$

where M is the molar mass of the volatile species, G the gas constant and T temperature, which is assumed to be constant.

The concentration gradient is obtained from the diffusion–advection equation for volatiles in the liquid:

$$\frac{\partial C}{\partial t} + \frac{\partial C}{\partial r} v_{liq} = \frac{1}{r^2}\frac{\partial}{\partial r}\left(Dr^2 \frac{\partial C}{\partial r} \right). \tag{2.27}$$

The equation is subjected to two boundary conditions. From the mass conservation requirement, we allow no volatile mass flux across the outer cell boundary:

$$\left. \frac{\partial C}{\partial r} \right|_{r=S} = 0. \tag{2.28}$$

The boundary condition at the bubble interface relates the concentration of volatiles to gas pressure through Henry's solubility law (evaporation is assumed to be instantaneous):

$$C(r = R, t) = K_H P_{gas}^{1/n}. \tag{2.29}$$

The radial growth of the bubble and the gas pressure in the bubble are obtained by simultaneous solution of the equations of motion (2.24) and the equations of

volatile mass transfer (2.25) and (2.21), (2.27)–(2.29). These equations are coupled, as the boundary conditions of both volatile diffusion and viscous resistance depend on P_{gas}. This set of equations requires numerical solutions (e.g. Proussevitch *et al.* 1993; Lyakhovsky *et al.* 1996). Analytical solutions for growth, where the effects of mass transfer and viscous resistance are de-coupled, were obtained by Navon, Chekhmir & Lyakhovsky (1998) and Lyakhovsky *et al.* (1996) and will be discussed below in relation to bulk viscosity.

3. Bulk viscosity solutions

To understand the dynamic behaviour of the expanding suspension, we calculate and draw its unloading path, i.e. its path in the space of driving pressure and strain rate. We consider a suspension that is suddenly decompressed to P_{amb} from the initial saturation pressure (P_0 when no bubbles present and P_i when bubbles of radius R_i are initially equilibrated).

First we demonstrate that our approach to determining bulk viscosity (equation (2.12)) reproduces the solutions of bulk viscosity for the case of no mass flux (equation (1.1)). We use the same assumptions as were used by Taylor (1954) in equation (1.1): the mass of gas and its temperature are constant ($PV = \text{const.}$), the gas volume fraction is low, surface tension is negligible and the shear viscosity of the incompressible liquid is uniform. As was shown, the driving pressure in a non-exsolving suspension is $P_{drive} = P_{gas} - P_{amb}$. In these conditions the expansion strain rate (equation (2.13)) is governed only by the viscous resistance of the liquid around the bubble, which is represented by (2.24). Substitution of (2.24) and (2.13) and P_{drive} from above into (2.11) reproduces equation (1.1):

$$\zeta = \frac{\mathrm{d}(P_{gas} - P_{amb})}{\mathrm{d}\left(\frac{3\alpha}{4\eta}(P_{gas} - P_{amb})\right)} = \frac{4}{3}\frac{\eta}{\alpha}. \tag{3.1}$$

Now, we allow gas influx from the supersaturated liquid into the bubbles (the pressures of both systems were presented in § 2.2). Three governing factors control the dynamics of bubble growth from a supersaturated liquid (§ 2.5):

(i) the resistance of the viscous liquid to bubble expansion (equation (2.24));

(ii) the efficiency of volatile diffusion (equations (2.25), (2.27)–(2.29));

(iii) the size of the liquid shell containing oversaturated volatiles (equation (2.14)).

Figure 2 shows a typical growth path, calculated numerically, and the three analytical end-member solutions. The example given is of a vesiculating magma, where the liquid is a silicic melt, the dissolved volatile is water and the rest of parameters are listed in table 1. We chose this system because of its significance in volcanic processes and because it is well-constrained by experimental studies (see the review by Navon & Lyakhovsky 1998). Below, we describe the three bubble growth regimes and present the respective expression for the bulk viscosity in each regime.

3.1. *Stage 1 – expansion controlled by the viscous resistance of the liquid*

In the initial stages, immediately after decompression, bubbles are still small enough so that the diffusive flux of volatiles keeps the gas pressure in equilibrium with the supersaturated melt and prevents fast fall of gas pressure. Initially, bubbles of radius R_i are equilibrated under pressure P_i (in practice $P_i = P_0$). The ambient pressure suddenly drops and consequently the now supersaturated liquid exsolves water to the expanding bubbles and maintains $P_{gas} \approx P_i$. The viscous resistance of the liquid (equation (2.24)) is the limiting process that governs the rate of bubble expansion.

Initial radius	$R_i = 0.1\,\mu\text{m}$
Initial cell size	$S_i = 54\,\mu\text{m}$
Initial water concentration	$C_i = 0.05$
Initial supersaturation pressure	$P_i = 150\,\text{MPa}$
Ambient pressure	$P_{amb} = 120\,\text{MPa}$
Temperature	$T = 800\,^\circ\text{C}$
Diffusivity of water in the melt	$D = 10^{-12}\,\text{m}^2\,\text{s}^{-1}$
Shear viscosity of the melt	$\eta = 5\,10^8\,\text{Pa}^1\,\text{s}^1$
Gas constant	$G = 8.314\,\text{J}\,\text{mol}^{-1}\,\text{K}^{-1}$
Henry constant	$K_H = 4\,10^{-6}\,\text{Pa}^{-0.5}$
Power of pressure in Henry's law	$n = 2$
Viscous time scale	$\tau_v = \eta/\Delta P \approx 17\,\text{s}$
Diffusive time scale	$\tau_d = S_0^2/D \approx 3000\,\text{s}$

TABLE 1. Parameters of the numerical simulations.

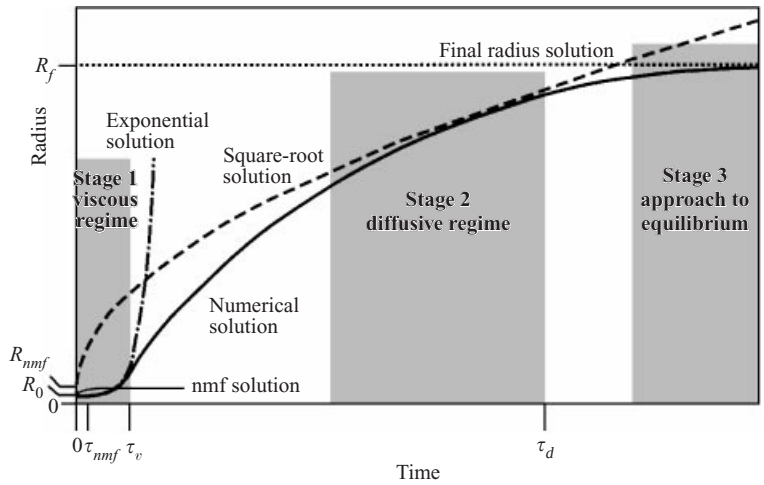

FIGURE 2. Bubble growth from a supersaturated magma under constant ambient pressure. The numerical solution (thick solid curve) is presented along with three asymptotic solutions (equations (3.2), (3.5) and (3.7)). The exponential solution (dashed-dotted curve) fits well the numerical solution for $t < \tau_v$ (stage 1). At longer times, but still shorter than the diffusive time scale (stage 2), the numerical solution approaches the square-root approximation. Growth ceases when the melt shell approaches saturation, at $t \gg \tau_d$ (stage 3). Also shown (thin solid curve) is the solution for the case of growth with no mass flux (nmf). The bubble grows to a smaller final size compared with the numerical case ($R_{f\_nmf} < R_f$) and on a shorter time scale $\tau_{nmf} = \tau_v(P_0 - P_{amb})/P_{amb}$.

Integrating (2.24), assuming low gas volume fraction ($\alpha \ll 1$), negligible surface tension, and constant viscosity (due to the relatively flat water concentration profile), yields the exponential growth law:

$$R = R_i \exp\left(\frac{t}{\tau_v}\right), \tag{3.2}$$

$$\tau_v = \frac{4\eta}{P_i - P_{amb}}. \tag{3.3}$$

Navon *et al.* (1998) verified the exponential growth law (3.1) experimentally. The exponential growth continues as long as P_{gas} remains close to P_i, which is when

$t < \tau_v$. At later times, P_{gas} relaxes and falls from P_i to P_{amb} and consequently bubble growth decelerates (compare with the numerical solution in figure 2).

During this stage the solubility pressure continuously decreases (equation (2.15)), as volatiles are exsolved from the liquid. Thus, the driving pressure relaxes, while the expansion strain rate increases. Substitution of (3.2) into (2.18) yields an approximately constant bulk viscosity with negative sign:

$$\zeta \approx -\frac{P_i n \tau_v}{3} \frac{\rho_{gas}}{\rho_{liq} C_i}. \tag{3.4}$$

3.2. *Stage 2 – expansion controlled by the rate of volatile diffusion*

At longer times, $t \gg \tau_v$, as bubbles expand and the surface/volume ratio decreases, diffusive flux of water cannot maintain the gas pressure close to the initial saturation pressure (P_0). The gas pressure then falls to slightly above ambient pressure. At this stage, bubble growth is impeded by the diffusive flux of water into the bubble. When diffusion is quasi-static (low Péclet number) and the volatile concentration at S is still close to the initial value ($C_{r=S} \sim C_{t=0}$), equation (2.27) gives the concentration gradient at the bubble interface $(\partial C/\partial r)_R = (C_0 - C_R)/R$ (Lyakhovsky *et al.* 1996). Substitution of this gradient into the equation of volatile mass balance (2.25) yields the square-root growth law

$$R = \sqrt{D_{eff} t}, \tag{3.5}$$

where the effective diffusivity is $D_{eff} = 2D\rho_{liq}(C_0 - C_R)/\rho_{gas}$.

The square-root solution is applied after the gas pressure drops to slightly above ambient pressure, and continues while $\alpha \ll 1$ and until diffusion starts to deplete the dissolved volatiles from the cell boundary (i.e. $C_S < C_0$). This occurs before reaching the characteristic time scale for diffusion $\tau_d \approx S_0^2/D$, which expresses the time it takes to diffuse water from the cell boundary to the bubble interface (i.e. when $\tau_v \ll t < \tau_d$).

The analytical solution of bulk viscosity at the diffusive regime, obtained by substitution of (3.5) into (2.18), is a negative linear function of time:

$$\zeta \approx -2P_0 n \frac{\rho_{gas}}{\rho_{melt} C_0} t. \tag{3.6}$$

Bulk viscosity is still negative under the conditions of the square-root solution. At longer times, $t > \tau_d$, the diffusive flux diminishes and the expansion strain rate decreases and thus the bulk viscosity becomes positive, as will be discussed in § 3.4.

3.3. *Stage 3 – finite shell and approach to equilibrium*

In a multi-bubble system (figure 1) equilibrium is attained when the excess volatiles are transferred into the bubble, i.e. when the solubility pressure approaches ambient pressure ($P_{sol} \sim P_{amb}$). This occurs when $t \gg \tau_d$. The radius of the bubble in equilibrium is determined by consideration of volatile mass conservation (equation (2.14)),

$$R^3 = S_0^3 \frac{\rho_{liq} G T K_H}{M} \left(\frac{P_0^{1/n} - P_{amb}^{1/n}}{P_{amb}} \right). \tag{3.7}$$

Bulk viscosity has no meaning when the fluid is at rest. When approaching equilibrium, the system relaxes and the driving pressure ($P_{sol} - P_{amb}$) decreases to a negligible value; so does the expansion strain rate. There is no simple analytical solution for this stage and we only show that the sign of bulk viscosity is positive (figure 4, when $t \gg \tau_d$).

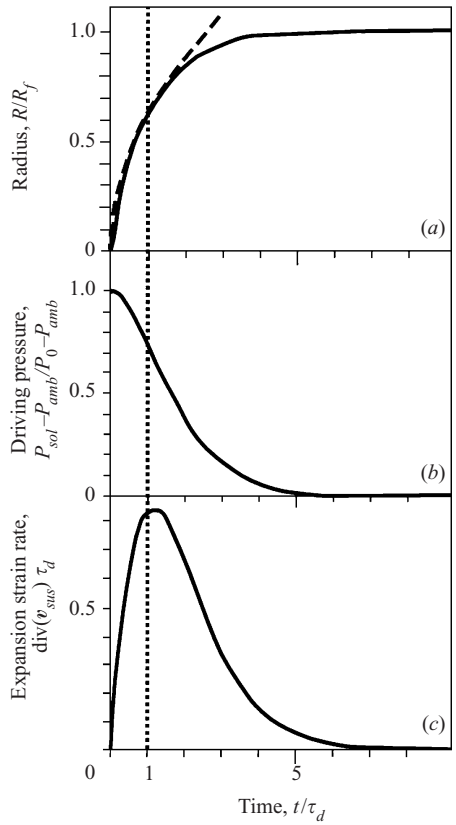

FIGURE 3. Expansion dynamics based on the two-phase cell model (see table 1 for list of parameters). (*a*) Bubble radius. The square-root approximation (dashed curve) follows the numerical solution (solid curve) until the diffusive time scale $\tau_d = S_0^2/D \sim 3000$ s. The viscous time scale is too short to be presented in this diagram ($\tau_v \sim 0.02\tau_d$). (*b*) The driving pressure ($P_{sol} - P_{amb}$) continuously decreases from the initial supersaturation pressure to zero when $t > 5\tau_d$. (*c*) The expansion strain rate ($\mathrm{div}\,\boldsymbol{v}_{sus}$) reaches a maximum shortly after $t \sim \tau_d$. At $t > \tau_d$, expansion decelerates, and approaches zero when $t > 5\tau_d$.

At equilibrium, the volume of the bubble is proportional to the volume of the surrounding melt (S_0^3). When approaching equilibrium, the shell size (S) is a sensitive parameter of the model. If the 'observation time' is comparable to or longer than the diffusive time scale then small variations in the choice of the cell size will influence the bubble size. Otherwise, when the diffusive time scale is longer than the observation time, then shell size is effectively infinitely large and one of the two solutions (equations (3.2) and (3.5)) may describe the growth path. The typical shell size, S, in silicic magmas is in the range 10^{-5}–10^{-2} m, corresponding to bubble number density of 10^5–10^{15} bubbles per cubic metre.

3.4. *Dynamic evolution of the expanding cell – numerical solutions*

We solve for the dynamic evolution of the expansion of the suspension under the control of the three governing factors (diffusion, viscous resistance and finite liquid reservoir). We obtain the evolution of the driving pressure, expansion strain rate and bulk viscosity by substitution of the solutions of the bubble growth evolution into (2.13), (2.17) and (2.18) respectively. We modified the numerical code of Lyakhovsky

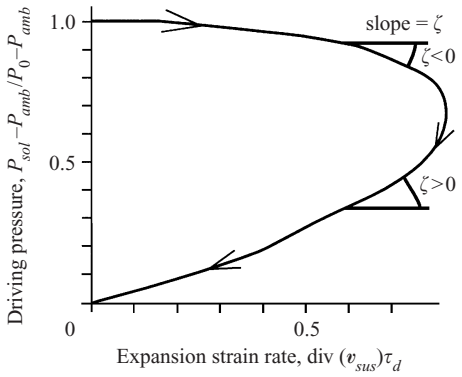

FIGURE 4. Driving pressure vs. expansion strain rate for expanding magma based on the two-phase cell simulations (figure 3). The slope of the curve is the bulk viscosity. Note that expansion begins with negative bulk viscosity, driving pressure decreases (figure 3*b*), while the expansion strain rate increase (figure 3*c*). The transition from negative to positive bulk viscosity occurs after about the diffusive time. The enclosed area represents the work done by the cell (4.5). The initial supersaturation pressure and the diffusive time are used for scaling the driving pressure and the strain rate.

et al. (1996), which solves the set of equations of the two-phase cell model, to calculate the radius of a growing bubble and the pressure in it.

Figure 3 follows the evolution of bubble growth, the driving pressure of the cell and the expansion strain rate (see table 1 for parameters). As the bubble grows, volatiles exsolve and the driving pressure drops. The expansion strain rate initially increases and reaches maximum shortly after $t \sim \tau_d$ and from then on the strain rate relaxes towards equilibrium. The time of maximum expansion strain rate relates to the estimated time for maximum gas influx, i.e. about $t \sim \tau_d$. When $t > \tau_d$, the expansion strain rate decreases, and when $t > 5\tau_d$, the system is almost relaxed; the bubble reaches its final radius ($R \sim R_f$), the solubility pressure is close to ambient pressure ($P_{sol} \sim P_{amb}$) and the strain rate vanishes ($\mathrm{div}(v_{sus}) \sim 0$).

Figure 4 follows the unloading path of the one-phase cell on a driving pressure–strain rate diagram. The slope of the curve is the bulk viscosity. Note that expansion begins with negative bulk viscosity and continues with positive sign. The sign inversion occurs when the expansion rate reaches its maximum at about the diffusive time scale (figure 3*c*). Until the diffusive time, gas flux is high enough to drive accelerated expansion even though the driving pressure decreases (figures 3*b* and 3*c*). From then on, expansion decelerates as expected from a dissipative system.

The analytical solutions for the bulk viscosity closely follow the numerical simulation under relevant conditions (figure 5). When $t < \tau_v$ (exponential bubble growth), bulk viscosity is constant both in the analytical solution and in the numerical solution, with less than 10% deviation between the solutions (figure 5*a*). At $\tau_v \ll t < \tau_d$ (square-root growth law), bulk viscosity is negatively linear with time (figure 5*b*). At later times, $t > \tau_d$, the system relaxes toward equilibrium. Both the driving pressure and the strain rate decrease with time and the bulk viscosity is positive (figures 3 and 4). The sign of the bulk viscosity and energetic considerations will be discussed in § 4.2.

In the next section we discuss the significance of negative bulk viscosity in volcanic conduits, focusing on the limit of short observation time, i.e. infinite shell size.

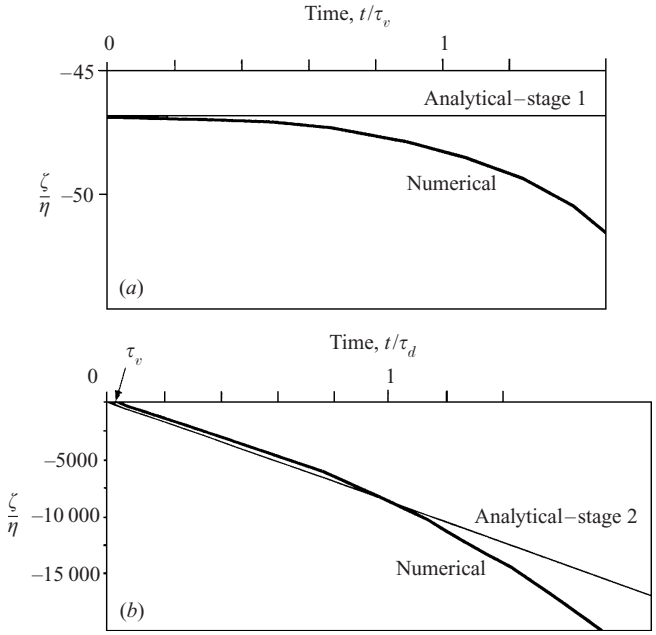

FIGURE 5. Bulk viscosity vs. time. The calculation uses the parameters listed in table 1. (*a*) During stage 1, at $t < \tau_v$, the bulk viscosity is negative and deviates by less than 10% from the analytically calculated value (3.4). Time is scaled to τ_v and bulk viscosity is scaled to the melt shear viscosity. (*b*) During stage 2, when $\tau_v < t < \tau_d$, the bulk viscosity is negative and the numerical solution follows the linear approximation of the analytical solution (3.6).

4. Discussion

The flow of bubbly suspensions is a complex phenomenon. Its mathematical description requires the determination of the constitutive relations (including bulk viscosity). For example, Massol & Jaupart (1999) have demonstrated that significant pressure gradients are expected to develop across the conduit due to the compressibility of the magma. Here we have derived expressions for bulk viscosity accounting for the exsolution of supersaturated volatiles into the growing bubbles. We use the numerical values of the bulk viscosity to evaluate the amplification of waves in the passage of a decompression front through a compressible magma due to a negative bulk viscosity.

4.1. *Amplification of rarefaction waves along volcanic conduits*

Active volcanic conduits, filled by volatile-bearing magma, are known to amplify seismic waves. The amplification was recently attributed to the effect of a 'wave trap', caused by the shape of the conduit and the contrasting seismic velocities across the conduit walls (Neuberg *et al.* 2000). This effect was calculated under the assumption that, in the relevant time scale, magma is purely elastic with respect to compressional waves (i.e. the amplitude of the waves is not attenuated by the compressible magma). Waves travelling through a visco-elastic fluid are attenuated due to viscous dissipation. However, if the bulk viscosity is negative, the system amplifies the wave and the system is unstable. Volatile-saturated magma is expected to amplify expansion waves rather than attenuate them. This amplification mechanism may provide another explanation for the effects of wave amplification in volcanic conduits and the stability of volcanic conduits.

We wish to examine whether an expansion strain wave of initial amplitude ε_0 can

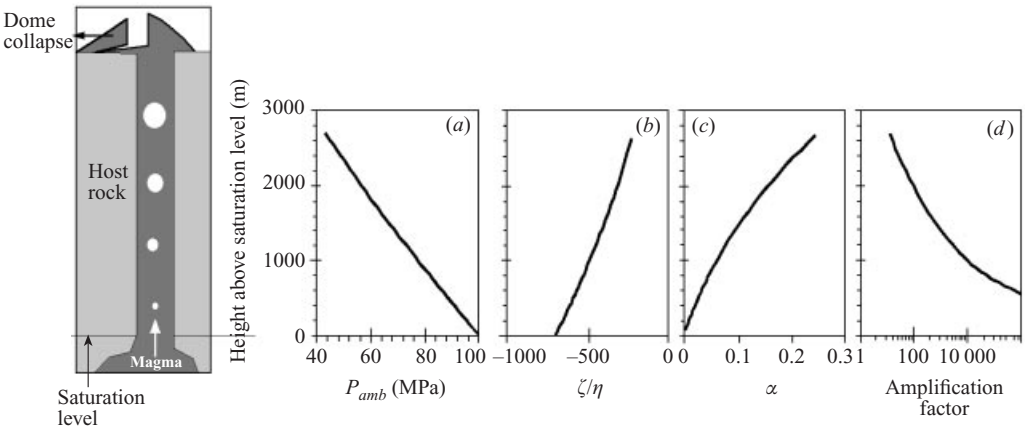

FIGURE 6. Amplification of a rarefaction wave along a conduit. (*a*) The ambient pressure profile along the conduit, i.e. magma-static pressure. (*b*) Bulk viscosity, in units of shear viscosity of the liquid, ζ/η. (*c*) Gas volume fraction. (*d*) Amplification factor. As the wave propagates downwards, it amplifies exponentially, and at some level the walls of the conduit will not resist the high strains. Conduit failure occurs when the product of the initial strain amplitude and the amplification factor is higher than the strength of the conduit walls ($\varepsilon_0 \exp(Lv_p\rho_{sus}/\zeta) \gg E$).

be amplified to such levels that the conduit walls are damaged, i.e. a critical strain, ε_{cr}, that the wall rocks cannot resist, is exceeded.

Consider a narrow volcanic conduit fed by magma with initial water concentration C_0. As the magma rises it decompresses and degasses by growing bubbles. If the ascent is slow enough, as is the case during the formation of lava domes (e.g. the present activity in Montserrat and Popocatepetl) the bubbles grow to equilibrium with the ambient magma-static pressure. Gas exsolution starts once the magma-static pressure is lower than the saturation pressure corresponding to C_0. Bubbles continue to grow as they move with the magma to higher levels (lower pressure). We assume a static magma column (figure 6) with equilibrium gas volume fraction increasing up the conduit and magma density decreasing upwards. If, for some reason, the ambient pressure suddenly drops at $t = 0$, the pre-existing bubbles start expanding and additional water exsolves from the now supersaturated melt into the bubbles. As shown in § 3.1, the expansion of bubbles (and the suspension) is roughly exponential at the initial stages ($t < \tau_v$, usually < 10 s) and the bulk viscosity of the suspension at this stage is negative.

In many cases, the dome above the conduit is gravitationally unstable. When part of it collapses, a rarefaction wave front travels down the conduit with initial amplitude ε_0. On travelling through a visco-elastic fluid, the amplitude of the expansion strain wave induced by such a front is attenuated with time by a factor

$$\exp\left(-\frac{\mu}{\zeta}t\right). \tag{4.1}$$

ζ/μ is the ratio of the bulk viscosity to the bulk modulus of the fluid and refers to the dilatational Maxwell time. However, in the case of a saturated conduit, ζ is negative and the expansion strain amplifies exponentially with time (equation (4.1)). The strain induced by the rarefaction wave increases while propagating down the conduit.

The time, t, available for amplification is determined by the length of the 'negatively

viscous' conduit, L, and by the wave velocity, v_p:

$$t \sim L/v_p. \tag{4.2}$$

L is measured from the depth of nucleation ($\sim$ saturation level) up to the place where magma is highly foamed and the bulk viscosity is no longer negative even at short times. The amplification at any depth is limited by both the duration of the negative viscosity regime (conservatively estimated as $t < \tau_v$), and by the period of the expansion wave. The bulk viscosity of silicic magma with water bubbles ($n = 2$) is

$$\zeta \approx -3\eta \frac{\rho_{gas}}{\rho_{liq} C_0} \frac{P_0}{\Delta P},$$

and the bulk modulus is

$$\mu \sim v_p^2 \rho_{sus}. \tag{4.3}$$

The condition for damage to the conduit walls, using equations (4.1)–(4.3) is

$$\exp\left(-L \frac{v_P \rho_{sus}}{\zeta}\right) > \frac{\varepsilon_{cr}}{\varepsilon_0}. \tag{4.4}$$

As shown in figure 6(*d*) the amplification factor increases rapidly and may be exceeded at depth.

This model is preliminary; however it shows that the effect of wave amplification is important in volcanic conduits containing saturated bubble-bearing magmas. Combining the amplification effects of the 'wave trap' (Neuberg *et al.* 2000) and the 'amplifying magma' may provide a better explanation for the triggering of the long period (LP) earthquakes that are observed in many volcanic centres and are used in monitoring volcanoes and to forecast eruptions. Similar effects may amplify rarefaction fronts initiated by major collapse of a volcanic dome and could trigger an eruption. Moreover, such conduits are sometimes unstable in the sense that decompression events, such as landslides, result in an explosive eruption (Melnik & Sparks 1999). The energy of explosive eruptions derives mostly from the exsolution of volatiles resulting from the decompression of magma.

4.2. *Negative bulk viscosity and energy balance*

In most closed mechanical systems, viscosity is positive, in accordance with the concept of viscous dissipation and the second law of thermodynamics (Landau & Lifshitz 1959; Batchelor 1967). Positive viscosity means that kinetic energy is dissipated to molecular motion and finally to heat. During expansion of bubble-bearing viscous melts, bulk viscosity is positive in the case of no volatile flux between the melt and the gas bubble (Taylor 1954). In a supersaturated magma, the potential energy of the excess dissolved volatiles in the melt is converted to expansion work of the gas. In some situations, only part of this energy dissipates to heat via the deformation of the viscous melt shell. In the presentation of the expanding magma as a single uniform phase the supersaturation and the associated potential energy can be accounted for by the magma pressure and bulk viscosity. The sign of the bulk viscosity depends primarily on the net mechanical power. It is negative when the dissipation of mechanical energy to heat is lower than the rate of conversion of potential energy of dissolved volatiles to expansion work. Other systems where the effective viscosity is negative are discussed in Starr (1968).

The change in the mechanical energy per mass unit (E_{sus}) of the compressible cell

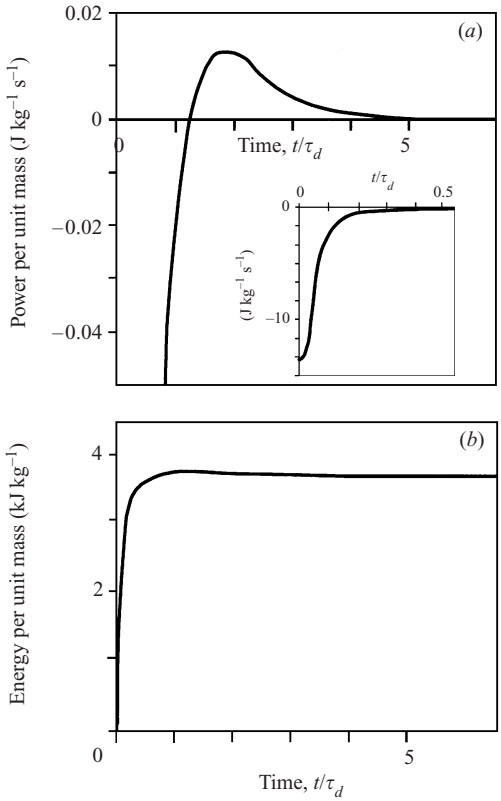

FIGURE 7. (*a*) Mechanical power of the expanding cell and (*b*) the energy of expansion, over time.

is the integral of power of the cell (W_{sus}) over time:

$$E_{sus}(t) = -\int_0^t W_{sus}\,\mathrm{d}t' = -\int_0^t \frac{1}{\rho_{sus}}(P_{sus} - P_{amb})\mathrm{div}\,v_{sus}\,\mathrm{d}t'. \tag{4.5}$$

Figure 7(*a*, *b*) presents the power and energy of an expanding cell (4.5) under the conditions listed in table 1. The mechanical power is negative as long as the rate of added work by volatile exsolution is higher than viscous dissipation, roughly when $t < \tau_d$ (figure 6*b*). At longer times, when volatile supply is too slow, the net power changes sign to positive, and the system dissipates energy. During the whole expansion process, the total change in energy is positive (figure 6*b*), with only a small fraction of the expansion work being dissipated as heat.

5. Summary

(i) The dynamic behaviour of an expanding suspension with volatile exsolution into the bubbles significantly differs from the case of expansion without mass flux. When no volatiles are added, the expansion strain rate monotonically decreases with time, until the gas pressure is equal to ambient pressure. Bulk viscosity is positive, as both the driving pressure and the expansion strain rate decrease with time. However, when volatiles exsolve into the bubbles, the expansion strain rate increases initially while the driving pressure decreases. The effective bulk viscosity in this period is negative.

The expressions for the bulk viscosity of the suspension with no volatile mass flux are not applicable for suspensions that exsolve volatiles.

(ii) Expressions for the bulk viscosity of volatile exsolving suspensions are derived in terms of the evolution of the radius of the bubbles and the gas pressure within them. We present simplified analytical solutions of the bulk viscosity in two end-member regimes, where analytical solutions of bubble growth are obtained. Numerical solutions of the bubble growth model are used to follow the variation in bulk viscosity and average density during the whole course of expansion.

(iii) A compressible fluid (suspension) with negative viscosity may amplify strains induced by rarefaction fronts. Such a situation may occur in volcanic conduits filled with water-saturated magma. The collapse of a volcanic edifice at the top of an active conduit sends a decompression front down the conduit. As the bulk viscosity at the initial stage is negative, the rarefaction wave is amplified as it travels downwards. Below a certain depth, the amplification may be large enough to break the conduit walls and initiate a volcanic event.

(iv) New analytical solutions were derived for the case of constant ambient and gas pressure. In these cases the bulk viscosity may be described using the parameters of the suspension, e.g. liquid properties, initial and final ambient pressure. In more general cases, the suspension may be obtained using numerical solutions of the two-phase bubble growth model.

We thank Oleg Melnik, Jurgen Neuberg and Amotz Agnon for useful discussions and suggestions, and Howard Stone, Steve Sparks and an anonymous reviewer for constructive reviews. Research was funded by the Israel–US Binational Science Foundation and in its late stage also by the EC MULTIMO project. N. G. L. acknowledges support by Yeshaya Horowitz Fellowship.

REFERENCES

Aksel, N. 1995 A model for the bulk viscosity of a non-Newtonian fluid. *Continuum Mech. Thermodyn.* **7**, 333–339.

Batchelor, G. K. 1967 *An Introduction to Fluid Dynamics*. Cambridge University Press.

Christensen, R. M. 1979 *Mechanics of Composite Materials*. John Wiley & Sons.

Dingwell, D. B. 1998 Recent experimental progress in the physical description of silicic magma relevant to explosive volcanism. In *The Physics of Explosive Volcanic Eruptions* (ed. J. S. Gilbert & R. S. J. Sparks), pp. 1–7. The Geological Society, London.

Landau, L. D. & Lifshitz, E. M. 1959 *Fluid Mechanics*. Addison-Wesley.

Lensky, N. G., Lyakhovsky, V. & Navon, O. 2001 Radial variations of melt viscosity around growing bubbles and gas overpressure in vesiculating magmas. *Earth Planet. Sci. Lett.* **186**, 1–6.

Lyakhovsky, V., Hurwitz, S. & Navon, O. 1996 Bubble growth in rhyolitic melts: Experimental and numerical investigation. *Bull. Volcanol.* **58**, 19–32.

Malvern, L. E. 1969 *Introduction to the Mechanics of a Continuous Medium*. Prentice-Hall.

Massol, H. & Jaupart, C. 1999 The generation of gas overpressure in volcanic eruptions. *Earth Planet. Sci. Lett.* **166**, 57–70.

Melnik, O. & Sparks, R. S. J. 1999 Nonlinear dynamics of lava dome extrusion. *Nature* **402**, 37–41.

Navon, O., Chekhmir, A. & Lyakhovsky, V. 1998 Bubble growth in highly viscous melts: theory, experiments, and autoexplosivity of dome lavas. *Earth Planet. Sci. Lett.* **160**, 763–776.

Navon, O. & Lyakhovsky, V. 1998 Vesiculation processes in silicic magmas. In *The Physics of Explosive Volcanic Eruptions* (ed. J. S. Gilbert & R. S. J. Sparks), pp. 27–50. The Geological Society, London.

Neuberg, J., Luckett, R., Baptie, B. & Olsen, K. 2000 Models of tremor and low-frequency earthquake swarms on Monserrat. *J. Volcanol. Geotherm. Res.* **101**, 83–104.

Proussevitch, A. A., Sahagian, D. L. & Anderson, A. T. 1993 Dynamics of diffusive bubble growth in magmas: Isothermal case. *J. Geophys. Res.* **98**, 22283–22307.

Prud'homme, R. K. & Bird, R. B. 1978 The dilatational properties of suspensions of gas bubbles in incompressible fluids. *J. Non-Newtonian Fluid Mech.* **3**, 261–279.

Rayleigh, Lord 1917 On the pressure development in a liquid during a collapse of a spherical cavity. *Phil. Mag.* **34**, 94–98.

Starr, V. P. 1968 *Physics of Negative Viscosity Phenomena.* McGraw-Hill.

Taylor, G. I. 1954 The two coefficients of viscosity for an incompressible fluid containing air bubbles. *Proc. R. Soc. Lond.* A **226**, 34–39.

Woods, A. W. 1995 The dynamics of explosive eruption. *Rev. Geophys.* **33**, 495–530.